

Spinal Cord Recordings in Rats During Skilled Reaching Task

Abhishek Prasad, *Student Member IEEE* and Mesut Sahin, *Senior Member IEEE*
Department of Biomedical Engineering, New Jersey Institute of Technology, NJ

Abstract- Descending signals in the rat cervical spinal cord (C5/C6) were recorded using a 15-channel microelectrode array during reach-to-grasp task. Signals were segregated into frequency bands to investigate the frequency content. Population activity was obtained by band-pass filtering the signals between 300Hz-3kHz. Local field potentials (LFPs) were analyzed between 0-13Hz, 13-30Hz, and 30-100Hz. The population activity and the LFPs in 0-13Hz were able to predict the behavior onset. Spectrograms indicated a clear difference between the quiet and behavioral state of the animal.

Keywords- principal component analysis, rubrospinal tract

I. INTRODUCTION

Electrophysiological experiments involving skilled reaching out to grasp an object task has been widely studied in rodents and primates [1-3]. Typically, these experiments rely on signals recorded from different regions of the motor cortex. Multiple cortical areas contribute uniquely to the control of the limb movement. It is difficult to record simultaneously from all these brain structures and study how the information is encoded and integrated within these regions. Motor signals descending in the spinal cord contain signals that have already undergone several levels of processing in the brain. In this study, we recorded descending signals in the rubrospinal tract (RST) at the cervical C5/C6 level in the rat spinal cord during skilled reach-to-grasp task. The RST, originating in the magnocellular division of the red nucleus [4], has been widely shown to be involved in the control of musculature producing skilled forelimb movements in rats and other species [5-8]. The cervical RST also receives inputs from the interpositus neurons that primarily control the forelimb movements, in rats [9-10] and other species [11], suggesting that information specific to the control of the forelimbs is available in the RST at the cervical level of the spinal cord [7].

In the spinal cord, each microelectrode records population activity from a pool of motor axons around its tip. The potentials recorded are related both to the axonal activity (source closer to the microelectrode) and the aggregate activity of the gray matter neurons (distant source). These two types of signals can be isolated based on frequency contents. Distant sources tend to occupy the low end of the spectrum [12-13] recorded locally as field potentials. The local field potentials (LFPs) can be obtained by using a low-pass filter with a cut-off of about 100Hz and a band-pass filter (300Hz-3kHz) can be used for obtaining axonal population activity. The axonal activity most probably represents the summation of potentials in the axon

bundles within a 50-300 μ m radius around the microelectrode tip [14]. LFPs represent low-frequency extracellular changes in voltages occurring due to synaptic activity [15], voltage-dependent membrane oscillations [16], and spike after-potentials that occur in the vicinity of the neural electrode. LFPs have been used to infer hand movements [17] and synchronous oscillations in LFP from the motor cortex have been found to be related to the aspects of movement preparation [18].

In this preliminary study, we investigated both the axonal activity and the LFPs in the spinal cord in terms of their frequency content and their ability to predict a skilled behavior.

II. EXPERIMENTAL SET-UP

A. Surgical Procedure

Two Long Evans male rats (300-350gms) were used in this preliminary study. All procedures were approved by the Institution of Animal Care and Use Committee (IACUC), Rutgers University, Newark, NJ. Rats were anesthetized by sodium pentobarbital (30mg/kg, IP) and additional doses of 6mg/kg were used when required during the surgical procedure. Dorsal laminectomy was performed at the cervical C5/C6 levels to expose the spinal cord. A custom-made 15-channel microelectrode array (Blackrock MicroSystems, UT) was implanted, under microscopic vision, into the dorsolateral funiculus at the C5/C6 segmental border of the rat spinal cord. The electrode was then fixed in its position using octyl cyanoacrylate tissue adhesive (Nexaband, WPI, Inc, FL). The microconnector was fixed to the skull using dental acrylic and screws.

B. Training and Recording Procedure

The rats were trained to reach through a small hole in a plexiglass box and grasp food pellets kept on a small tray. During recording, the rats were allowed to move freely inside the cage. A 32-channel, gain 10 headstage amplifier (TBSI Systems) was connected to the headstage microconnector on the animal. The amplifier was interfaced with the computer using a data acquisition card (National Instruments PCI6259). Five seconds of neural data as well as video images were acquired simultaneously using Matlab each time the rat performed the task. Both neural signals and video images were time stamped. Neural signals were acquired at a sampling rate of 30kHz and video images at 60 frames/s.

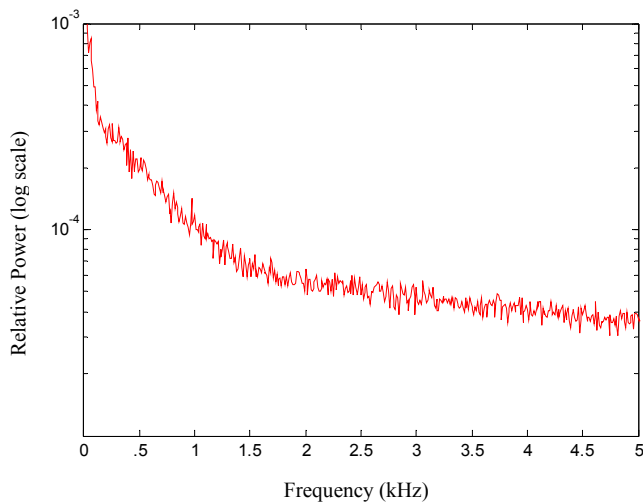


Fig. 1. Power spectrum of a typical neural channel.

III. DATA ANALYSIS

Matlab was used for data analysis. The power spectral density of a typical neural channel (Fig. 1) shows that there is a significant decrease in power after 3kHz and that the maximum power is concentrated below 1.5kHz. The filter cut-off frequencies were determined from the power spectrum plots.

LFPs were found to be contaminated with heart beats due to the selected frequency bands. Principal component analysis (PCA) was applied on the raw signal to remove the heart beat artifacts. In brief, fourier transform of the raw signal was used to determine the heart beat frequency and coherence between the raw signals and the principal components was done to find the component which contributed the heart beat artifact. The principal component (typically PC1) contributing to the heart beats was replaced by zeros and the principal components were back-projected to obtain the original neural signals. This method effectively removed the artifact from the LFPs.

Coherence was applied between all possible combination of adjacent electrode contacts and their average (Fig.2) was calculated to investigate the frequencies most commonly shared between the electrode channels. Then LFPs were segregated into separate frequency bands of 3-13Hz, 13-30Hz, 30-100, and 100-300Hz using a fourth order Butterworth filter for each of the bands. The population activity was band-pass filtered between 300Hz-3kHz. PCA was applied for LFPs and population activity to investigate if the behavior can be predicted using a fewer number of principal components (PCs). Spectrograms constructed using Welch technique was analyzed for evaluating the temporal distribution of frequencies in behaving and quiet animals.

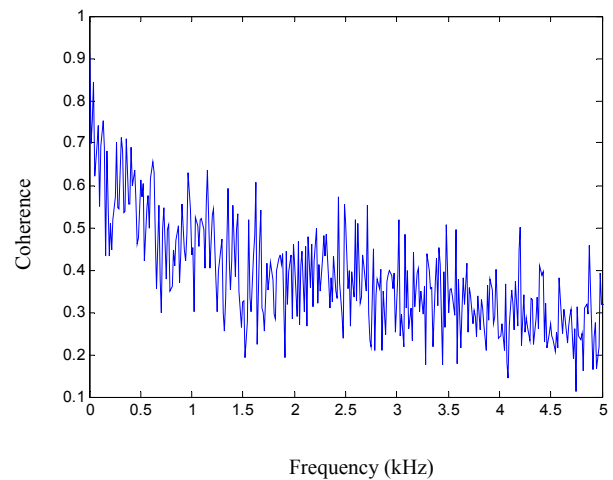


Fig. 2. Average coherence calculated between all possible combinations of the neural channels showing that coupling is stronger at the lower end of the spectrum in the LFP range.

IV. RESULTS and DISCUSSION

Coherence analysis suggested that the electrode channels shared frequencies that are less than 1kHz with a coherence of approximately 0.6 (Fig. 2). Electrode channels were more strongly coupled in the LFP frequencies. This suggests that each microelectrode shows higher spatial selectivity in recording of population activity than the LFPs. On the other hand the LFPs indicate the totality of potentials in a region. Such an overall effect is recorded by all the channels. The LFPs recorded in the spinal cord may be due to the neuronal activity occurring in the spinal cord gray matter which is not very far from the tips of the microelectrodes.

Fig. 3 shows a spectrogram plot of frequency varying as a function of time during the behavioral task and when the animal was quietly sitting. A clear shift in frequency can be observed between the two plots. An increase in frequency in the top plot coincides with the beginning of the reaching task (first peak at 0.5s) and the frequencies reduce when the animal acquired the food. The bottom plot is a spectrogram of the activity when the animal was quiet. There are only a few baseline frequency components and there is no variation as a function of time. The frequency shift in a spectrogram correlates well with the behavior and may be used for predicting behavior onset.

Fig. 4 shows the neural signals filtered within different frequency bands. The population activity (300-3kHz) always showed an increase during the behavior and decrease when the animal was quiet. The LFPs in the frequency range corresponding to 3-13Hz correlated well with the behavior and were able to predict the presence of behavior. LFPs in the 13-30Hz and 30-100Hz were not very well correlated with the behavior. However, signal components in the 100-300Hz and population activity (300-3kHz) were able to predict the behavior onset.

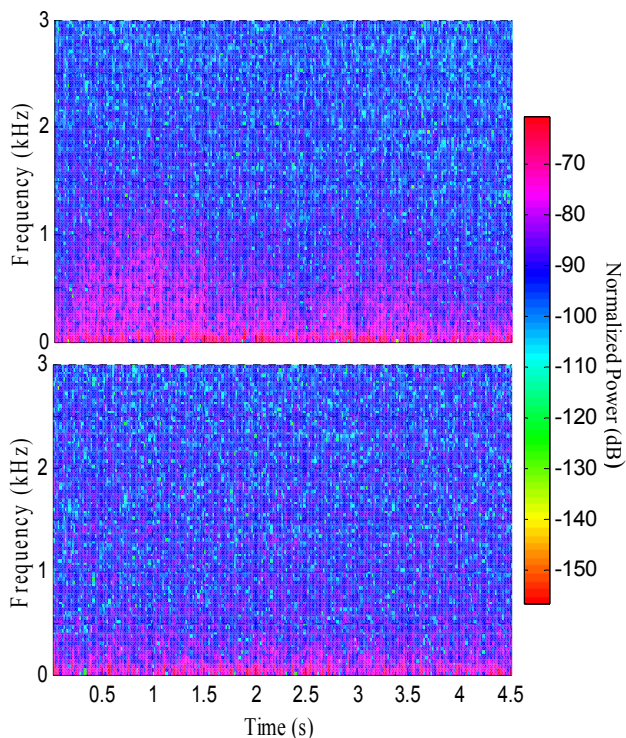


Fig. 3. Spectrogram estimated using Welch technique. The top plot shows the spectrogram while the animal was performing the behavioral task and the bottom plot shows while the animal was quiet.

The LFPs in the 13-100Hz range showed oscillations but these were not always correlated with the behavior. The oscillations also varied from one channel to the other. In general, the very slow changing LFPs, LFPs in the 100-300Hz range, and the population activity were able to correctly predict the onset and end of the behavior.

The peak-to-peak signal showed a clear differentiation of amplitudes in different frequency ranges (Fig. 4). The peak-to-peak signal amplitude for population activity was typically around $200\mu\text{V}$ whereas that for LFPs varied between $10\text{-}100\mu\text{V}$, with the slow frequency LFPs showing maximum peak-to-peak amplitude (Fig. 4).

PCA was used to reduce the dimensionality of the data and to investigate the number of PCs required to account for at least 90% of the variance in the data. Fig. 5(A) shows the percentage of variance accounted by each PC for LFPs. The first PC for LFPs accounted for approximately 50% of the variance in the data. Five or six PCs taken together accounted for at least 90% of the variance in the LFP data. However, for population activity, PC1 accounted for 70% of the variance and approximately 2-3 PCs could explain for 90% of the variance. In general, fewer PCs were required to account over two-thirds of the variance in the population activity. PC1 was also able to predict the onset of behavior in case of population activity whereas the PC1 for LFPs was not (Fig. 6). However, the large peak at the onset and other small peaks coincide with the activity in the first plot. This suggests that these peaks are due to the very slow LFPs which correlate well with the behavior onset.

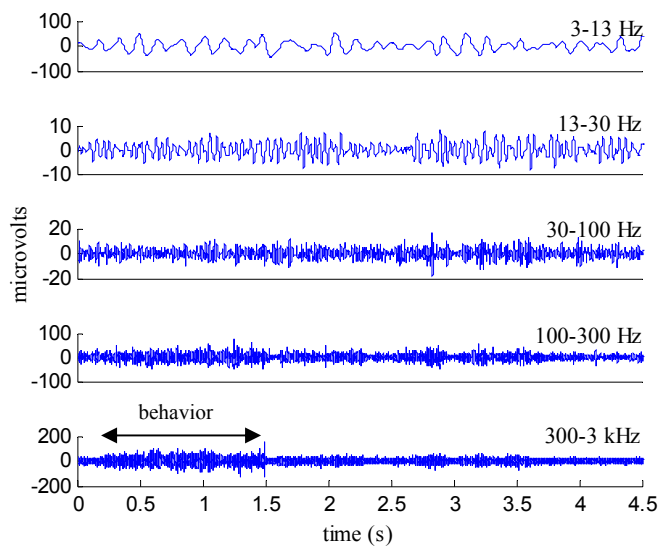


Fig. 4. A channel of neural signal separated into various frequency bands. Signal amplitudes shown are original amplitudes after dividing with the amplifier gain.

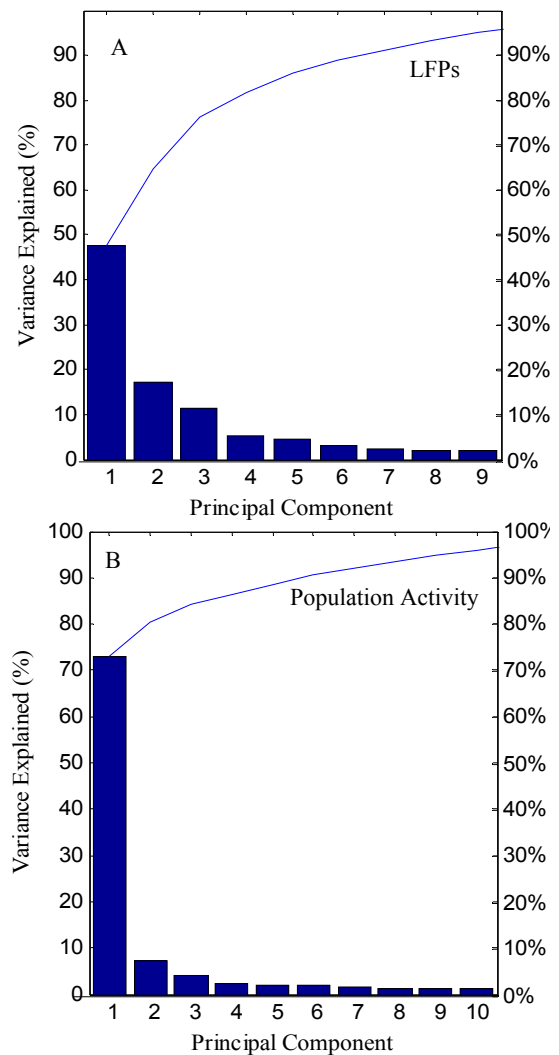


Fig. 5. Variances accounted by each principal component after PCA. The top plot (A) is for LFPs and the bottom plot (B) is for population activity.

ACKNOWLEDGMENT

This study was supported by a NIH grant R21 NIH/NICDS HD056963-01 A2. The authors would also like to thank Nicholas Sachs, PhD for helping during surgery and recording sessions.

REFERENCES

- [1] J. M. Carmena, M. A. Lebedev, R. E. Crist *et al.*, "Learning to control a brain-machine interface for reaching and grasping by primates," *PLoS Biology*, vol. 1, no. 2, 2003.
- [2] J. P. Donoghue, J. N. Sanes, N. G. Hatsopoulos *et al.*, "Neural discharge and local field potential oscillations in primate motor cortex during voluntary movements," *Journal of Neurophysiology*, vol. 79, no. 1, pp. 159-173, 1998.
- [3] B. Hyland, "Neural activity related to reaching and grasping in rostral and caudal regions of rat motor cortex," *Behavioural Brain Research*, vol. 94, no. 2, pp. 255-269, 1998.
- [4] H. M. Murray, and M. E. Gurule, "Origin of the rubrospinal tract of the rat," *Neuroscience Letters*, vol. 14, no. 1, pp. 19-23, 1979.
- [5] I. Q. Whishaw, B. Gorny, and J. Sarna, "Paw and limb use in skilled and spontaneous reaching after pyramidal tract, red nucleus and combined lesions in the rat: Behavioral and anatomical dissociations," *Behavioural Brain Research*, vol. 93, no. 1-2, pp. 167-183, 1998.
- [6] P. L. E. Van Kan, and M. L. McCurdy, "Role of primate magnocellular red nucleus neurons in controlling hand preshaping during reaching to grasp," *Journal of Neurophysiology*, vol. 85, no. 4, pp. 1461-1478, 2001.
- [7] A. R. Gibson, K. M. Horn, M. Pong *et al.*, "Construction of a reach-to-grasp," *Novartis Foundation Symposium*, 1998, pp. 233-251.
- [8] H. Jarratt, and B. Hyland, "Neuronal activity in rat red nucleus during forelimb reach-to-grasp movements," *Neuroscience*, vol. 88, no. 2, pp. 629-642, 1999.
- [9] H. Daniel, J. M. Billard, P. Angaut *et al.*, "The interposito-rubrospinal system. Anatomical tracing of a motor control pathway in the rat," *Neuroscience Research*, vol. 5, no. 2, pp. 87-112, 1987.
- [10] M. C. Jiang, G. F. Alheid, M. G. Nunzi *et al.*, "Cerebellar input to magnocellular neurons in the red nucleus of the mouse: synaptic analysis in horizontal brain slices incorporating cerebello-rubral pathways," *Neuroscience*, vol. 110, no. 1, pp. 105-121, 2002.
- [11] F. R. Robinson, J. C. Houk, and A. R. Gibson, "Limb specific connections of the cat magnocellular red nucleus," *Journal of Comparative Neurology*, vol. 257, no. 4, pp. 553-577, 1987.
- [12] U. Mitzdorf, "Current source-density method and application in cat cerebral cortex: Investigation of evoked potentials and EEG phenomena," *Physiological Reviews*, vol. 65, no. 1, pp. 37-100, 1985.
- [13] G. Kreiman, C. P. Hung, A. Kraskov *et al.*, "Object selectivity of local field potentials and spikes in the macaque inferior temporal cortex," *Neuron*, vol. 49, no. 3, pp. 433-445, 2006.
- [14] D. A. Henze, Z. Borhegyi, J. Csicsvari *et al.*, "Intracellular features predicted by extracellular recordings in the hippocampus in vivo," *Journal of Neurophysiology*, vol. 84, no. 1, pp. 390-400, 2000.
- [15] U. Mitzdorf, "Properties of the evoked potential generators: current source-density analysis of visually evoked potentials in the cat cortex," *International Journal of Neuroscience*, vol. 33, no. 1-2, pp. 33-59, 1987.
- [16] A. Kamondi, L. Acsády, X. J. Wang *et al.*, "Theta oscillations in somata and dendrites of hippocampal pyramidal cells in vivo: Activity-dependent phase-precession of action potentials," *Hippocampus*, vol. 8, no. 3, pp. 244-261, 1998.
- [17] C. Mehring, J. Rickert, E. Vaadia *et al.*, "Inference of hand movements from local field potentials in monkey motor cortex," *Nature Neuroscience*, vol. 6, no. 12, pp. 1253-1254, 2003.
- [18] J. N. Sanes, and J. P. Donoghue, "Oscillations in local field potentials of the primate motor cortex during voluntary movement," *Proceedings of the National Academy of Sciences of the United States of America*, vol. 90, no. 10, pp. 4470-4474, 1993.

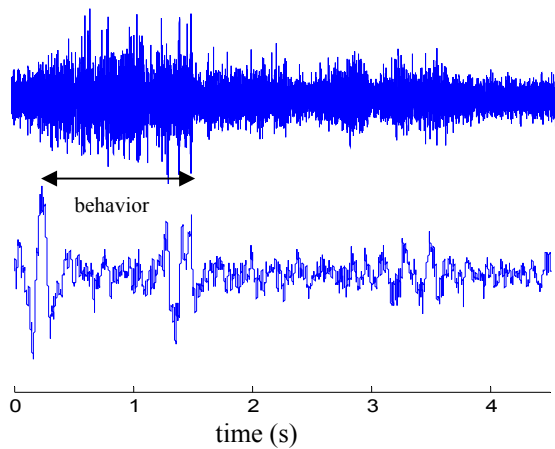


Fig. 6. The top plot shows the PC1 for the population activity. Note that there is an increase in the neural activity at around 0.5s which marks the onset of the behavioral task. The bottom plot shows the PC1 for the LFPs. The principal component for the LFP does not correlate with the timing of the behavior.

The animals were terminated after 4-6 weeks of recording and the spinal cord at the site of electrode was explanted for histology. Five micrometer thick sections of the spinal cord were stained by Luxol Fast Blue stain. The arrows show the location of electrode array (Fig. 7).

V. CONCLUSIONS

In this preliminary study, we have shown that descending signal in the spinal cord separated into different frequency bands can predict the presence of behavior involving forelimbs. The frequency content of the signals was studied and spectrograms were used to predict behavior onset and show difference in the frequency content of the signals in quiet and behaving animals. Principal component analysis was used to reduce the dimensionality of the signals and PC1 from population activity was found to increase with behavior with better accuracy than the PC1 from LFPs.

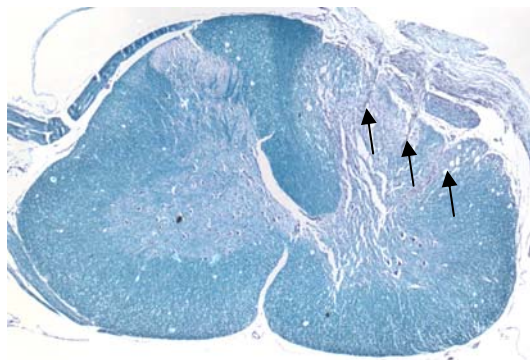


Fig. 7. A section of spinal cord stained using Luxol Fast Blue. The arrows indicate the location of microelectrode shanks.